Chinese Chemical Letters 35 (2024) 109736

Contents lists available at ScienceDirect

Chinese Chemical Letters

journal homepage: www.elsevier.com/locate/cclet

# Simple and versatile *in situ* thermo-sensitive hydrogel for rectal administration of SZ-A to alleviate inflammation and repair mucosal barrier in ulcerative colitis

Yu Yan [a,b,c,1], Jiawei Song [a,c,1], Dongdong Liu [a,b,c], Zihan Liu [a,c], Jialing Cheng [a,c], Zhiyang Chen [a,c], Yanfang Yang [a,c], Weizhe Jiang [b], Hongliang Wang [a,c,*], Jun Ye [a,c,*], Yuling Liu [a,c,*]

[a] *State Key Laboratory of Bioactive Substance and Function of Natural Medicines, Institute of Materia Medica, Chinese Academy of Medical Sciences & Peking Union Medical College, Beijing 100050, China*
[b] *College of Pharmacy, Guangxi Medical University, Nanning 530021, China*
[c] *Beijing Key Laboratory of Drug Delivery Technology and Novel Formulation, Institute of Materia Medica, Chinese Academy of Medical Sciences & Peking Union Medical College, Beijing 100050, China*

ARTICLE INFO

*Article history:*
Received 25 January 2024
Revised 1 March 2024
Accepted 5 March 2024
Available online 6 March 2024

*Keywords:*
Ulcerative colitis
SZ-A
Thermo-sensitive hydrogel
Rectal administration
Alleviation of inflammation
Mucosal barrier repair

ABSTRACT

Ulcerative colitis (UC) is a chronic inflammatory bowel disease characterized by persistent inflammation of the colon and disrupted intestinal function. *Ramulus mori* (Sangzhi) alkaloids (SZ-A), derived from twigs of mulberry, were approved by the National Medical Products Administration in 2020 for treating type 2 diabetes mellitus. Accumulated evidence has confirmed that SZ-A also alleviates non-alcoholic fatty liver disease and ameliorates inflammation, indicating its potential to address inflammation in UC. However, the treatment of UC faces challenges due to low drug delivery efficiency and short retention time. To overcome these challenges, an injectable and adherent *in-situ* thermo-sensitive hydrogel containing SZ-A was developed for rectal drug delivery, utilizing the thermo-sensitive polymers Poloxamer 407 and 188. The thermo-sensitive hydrogel system was designed with a moderate gelation temperature of 32 ± 0.5 °C, a short gelation time of 64 s, a pH range of 7–10, high moisturizing capability exceeding 90%, and moderate mechanical strength of 4–5 s. In a rat model with UC, the *in situ* thermo-sensitive hydrogel significantly extended the retention time at the colonic site and enabled sustained release after rectal administration. Symptoms of UC were markedly reduced following rectal administration of SZ-A thermo-sensitive hydrogel. Furthermore, the release of inflammatory factors, such as interleukin-1$\beta$ (IL-1$\beta$), IL-6, IL-18, tumor necrosis factor-$\alpha$ (TNF-$\alpha$), and transforming growth factor-$\beta$1 (TGF-$\beta$1), significantly decreased in the SZ-A thermo-sensitive hydrogel group. The integrity of the colonic mucosal barrier was significantly enhanced following the application of SZ-A thermo-sensitive hydrogel. In conclusion, rectal administration of SZ-A *in situ* thermo-sensitive hydrogel effectively alleviated UC symptoms, inhibited the secretion of inflammatory factors, and promoted the repair of the colonic mucosal barrier. This approach holds promise as a potential treatment for UC.



Ulcerative colitis (UC) is a prevalent intestinal ailment characterized by abdominal pain, diarrhea, and bloody mucous discharge [1–3]. UC often manifests alongside varying degrees of joint, skin, eye, liver, and bile damage, and in advanced stages, it may lead to malignancy [4–6]. Recent shifts in dietary and lifestyle patterns have contributed to a significant rise in the global incidence and prevalence of UC [7–9], establishing it as one of the most prevalent bowel diseases worldwide [10]. The pathogenesis of UC involves immune inflammation, oxidative stress, and cellular heat sink [11,12]. Clinical evidence indicates that ulcerative lesions coincide with heightened activation of the nuclear transcription factor-$\kappa$B (NF-$\kappa$B) signaling pathway, leading to the production of substantial pro-inflammatory cytokines, such as tumor necrosis factor-$\alpha$ (TNF-$\alpha$), interleukin-6 (IL-6), and IL-1$\beta$, along with compromised epithelial barrier function. Consequently, current clinical

* Corresponding authors.
*E-mail addresses:* wanghl@imm.ac.cn (H. Wang), yelinghao@imm.ac.cn (J. Ye), ylliu@imm.ac.cn (Y. Liu).
[1] These authors contributed equally to this work.

https://doi.org/10.1016/j.cclet.2024.109736
1001-8417/

approaches for UC primarily target inflammation reduction and hastening intestinal healing. Commonly employed drugs include 5-aminosalicylic acid, sulfasalazine, glucocorticoids, antibiotics, and immunosuppressants. However, their drawbacks include prolonged treatment duration, significant adverse reactions, and a high recurrence rate [13–15], stemming from their inability to specifically target colonic inflammation sites [16]. Furthermore, patients often experience severe side effects, such as nausea, headache, and hypertension [17,18]. Exploring anti-inflammatory compounds from traditional Chinese medicines presents a promising avenue for developing safe and efficacious UC treatments.

*Ramulus mori* (Sangzhi) alkaloids (SZ-A), a key component of traditional Chinese medicine derived from mulberry branches, constitute over 50% of the total extract. Mainly comprising 1-deoxynojirimycin, fagomine, and 1,4-dideoxy-1,4-imino-D-arabinitol, SZ-A exhibits highly selective inhibitory effects on small intestinal glycosidases [19]. Recognized for its efficacy in managing type 2 diabetes mellitus, SZ-A tablets received approval from the China National Medical Products Administration (NMPA) in 2020 (approval No. Z20200002). Beyond its proven hypoglycemic effects and safety profile, extensive research has revealed SZ-A's diverse pharmacological effects, including ameliorating lipid metabolism, mitigating inflammation linked to obesity, reducing insulin resistance, regulating gut microbiota disorders, and diminishing intestinal inflammation. These effects are attributed to the multitargeted actions of SZ-A's various components [20,21]. Focusing on SZ-A's anti-inflammatory properties, investigations have shown its ability to act on multiple inflammatory pathways, inhibiting the secretion of inflammatory factors, such as IL-1$\beta$, TNF-$\alpha$, and IL-6, and blocking p38 mitogen activated protein kinases (p38MAPK), extracellular signal-regulated kinases (ERK), and c-Jun N-terminal kinases (JNK) signaling pathways [22]. Given its established safety, anti-inflammatory efficacy, and impact on the intestinal flora, SZ-A holds promise as a highly effective and low-toxicity natural medicine for UC treatment.

Presently, SZ-A is commonly administered orally in tablet form for clinical treatment. However, this traditional dosage form encounters challenges in retaining active ingredients at the colonic site following oral administration. Furthermore, rectal administration of SZ-A solution results in the rapid efflux of active ingredients. The limited availability and brief retention time of SZ-A in colonic tissues significantly compromise its therapeutic efficacy in UC. Additionally, rectal administration of conventional dosage forms often necessitates a high volume and multiple delivery modes to achieve an effective therapeutic response. This can lead to secondary colonic mucosal damage and reduced intestinal sensitivity. Therefore, an urgent need exists to design an efficient delivery system for encapsulating SZ-A to increase its accumulation in the colon and enhance its therapeutic effect in UC.

Rectal drug delivery is a method in which drugs are administered through the anus into the intestinal canal to be released for efficacy in treating systemic or local diseases [23]. Compared with oral administration, rectal administration avoids direct stomach stimulation, which may cause symptoms such as nausea, vomiting, and gastric distension. Most drugs can be absorbed through the intestinal mucosa without passing through the liver, and entering the bloodstream directly, thereby reducing drug hepatotoxicity and associated side effects [24].

*In situ* thermo-sensitive hydrogels with solution-gel transition properties and strong bio-adhesiveness can rapidly gelate at body temperature, adhering widely to the surface of colonic lesions to enhance drug retention and therapeutic effects [25,26]. Following rectal administration of an *in situ* thermo-sensitive hydrogel, the hydrogel adheres quickly and tightly to the colonic mucosal surface. It then slowly dissolves under the influence of intestinal mucus, releasing encapsulated active ingredients to act on the colonic lesion and ultimately exert an anti-inflammatory effect [27,28]. Poloxamer 407 (P407), a thermo-sensitive material, is widely employed as a drug delivery vehicle, particularly as a thermo-sensitive hydrogel [29–31]. Comprising 70% polyoxyethylene units and 30% polyoxypropylene blocks [32,33]. P407 gradually dissolves into a low-viscosity solution as the temperature increases. This solution transforms into a semi-solid hydrogel by forming a network structure at temperatures close to body temperature. The gelation of P407 is highly dependent on polymer concentration [34]. Considered one of the safest polymer materials, P407 exhibits excellent biocompatibility [35,36]. Moreover, P407 hydrogels demonstrate good plasticity and adhesion, prolonging the residence time of drugs [37–39]. These characteristics position P407 as an attractive carrier for controlled drug delivery in various pharmaceutical applications.

In this study, we selected P407 as the thermo-sensitive material, Poloxamer 188 (P188) as the gelation temperature modulator, and hydroxypropyl methylcellulose (HPMC) as a bioadhesive material. These components were directly dissolved in an aqueous SZ-A solution to formulate a rectally administered *in situ* thermo-sensitive hydrogel for alleviating UC. The anticipated capability of the SZ-A thermo-sensitive hydrogel is to undergo a rapid transition from a liquid to a hydrogel, adhering to the colonic mucosa within the colonic lumen. This prolonged retention time of SZ-A is expected to enhance its therapeutic efficacy in UC. The hydrogel was initially optimized based on the gelation temperature using the star point response surface method. Subsequently, the concentrations of P407, P188, and HPMC in the hydrogel were further optimized, taking into account key parameters such as gelation time and the mechanical strength of the hydrogel. The physicochemical properties of the optimal formulation, including gelling time, temperature, pH, moisture retention properties, *in vitro* dissolution characteristics, and mechanical strength, were determined. Additionally, the retention of the SZ-A hydrogel in the colonic mucosa was investigated through *in vivo* imaging following rectal administration. Finally, a 2,4,6-trinitrobenzene sulfonic acid solution (TNBS)-induced UC rat model was established to assess the therapeutic effects of the SZ-A hydrogel on UC. These effects included the relief of typical symptoms, inhibition of inflammatory factor secretion, and repair of the colonic mucosal barrier.

The gelling temperature of a hydrogel denotes the temperature at which a thermo-sensitive gel undergoes the transformation from a solution to a gel. The temperature-sensitive SZ-A hydrogel was prepared using the cold solution method, as illustrated in Fig. 1A. Considering the gelation temperature as a criterion, a single-factor analysis was conducted to assess and determine the appropriate dosage range of the thermo-sensitive polymer P407, gelation temperature modulator P188, and bioadhesive polymer HPMC within the hydrogel. To align with the normal human body temperature range of 36–37 °C, the gel temperature was set at 32 °C, ensuring the temperature-sensitive gel was liquid at room temperature and quickly gelled at body temperature. Single-factor screening experiments revealed that under the ideal gelling temperature (32 °C), the suitable dosage ranges for P407, P188, and HPMC were 16%–18%, 2.5%–4%, and 0.3%–0.7%, respectively (Fig. 1B). Based on the optimization results from the single-factor experiments, further refinement of the formulation involving the dosages of P407, P188, and HPMC was performed using the Box-Behnken start-point response surface methodology with gelation temperature ($T$) as the response variable in a three-factor, three-level start-point design (Table S1 in Supporting information). With the gelation temperature set at 32 ± 0.5 °C, three representative hydrogel formulations were obtained and their gelation temperatures were validated and assessed using the simulation equation ($T = 35.26 - 3.22 \times A + 1.01 \times B - 0.89 \times C + 0.67 \times A \times B - 0.22 \times A \times C + 0.000 \times B \times C - 0.61 \times A^2 - 0.88 \times B^2 + 0.17 \times C^2$)

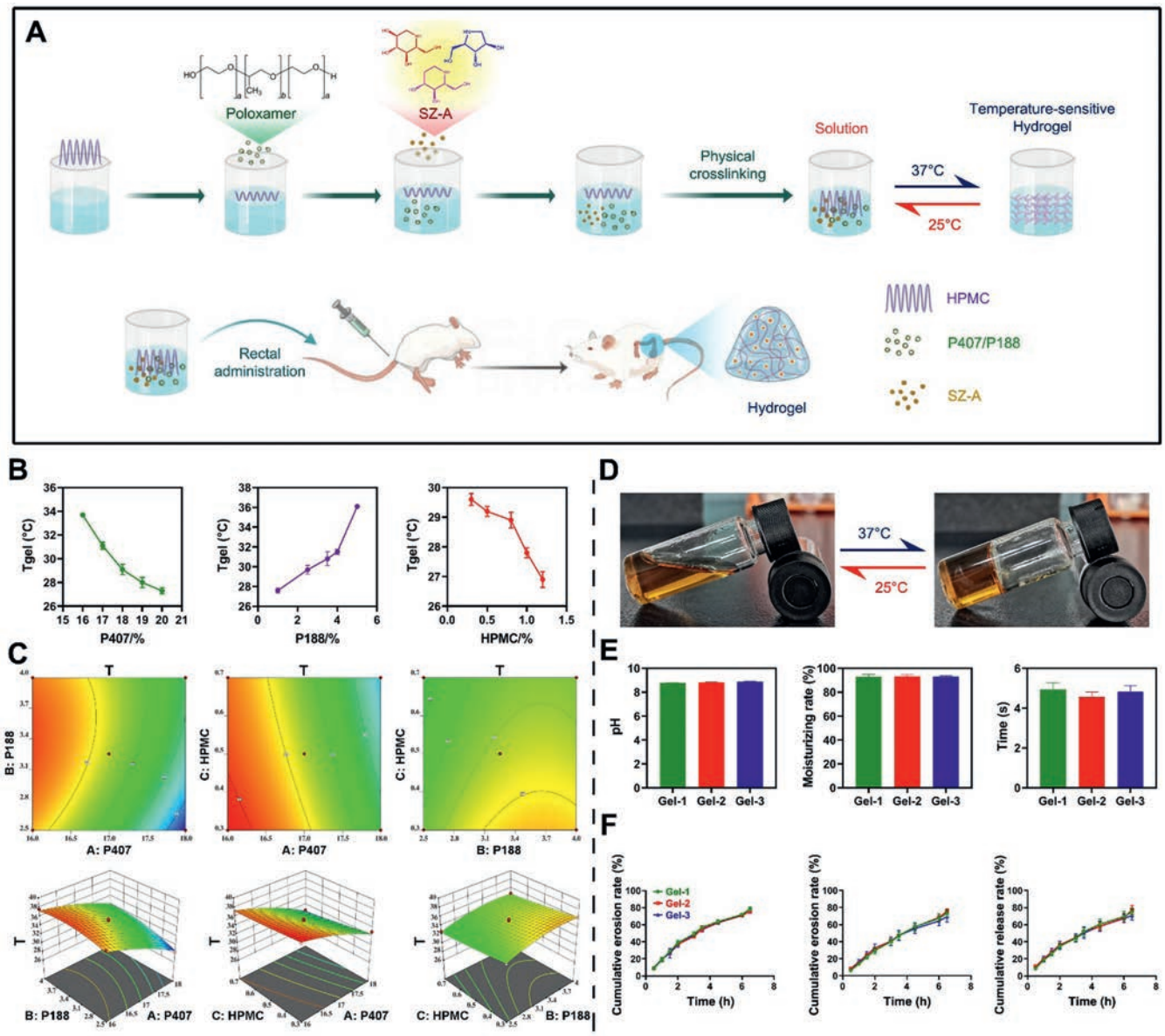


**Fig. 1.** Preparation and formulation optimization of thermosensitive gel: (A) Preparation process of thermosensitive gel. (B) Effect of different temperature-sensitive materials on gelling temperature. (C) Effect surface diagram and contour line diagram of influence of P407 dosage, P188 dosage and HPMC dosage on gelling temperature. (D) The macroscopic appearance of SZ-A hydrogel in response to temperature change. (E) Determination of pH, moisture retention, and gel strength of different SZ-A hydrogel. (F) Cumulative erosion rate of the blank gel, cumulative erosion rate/cumulative release rate of the drug. Data are presents as mean ± standard deviation (SD) ($n = 3$).

($R^2 = 0.9839$, $P < 0.0001$) (Fig. 1C and Table S2 Supporting information).

Physicochemical properties of the prepared hydrogels were characterized. At room temperature (25 °C), the three hydrogels appeared as clear and transparent brown solutions with good flowability. As the temperature reached the critical value of the gelation temperature (32 °C), all three hydrogels rapidly transformed into a uniform brown gel (Fig. 1D), demonstrating pronounced thermo-sensitive characteristics. The pH, moisture retention, and gel strength of the three thermo-sensitive hydrogels are depicted in Fig. 1E. The pH of all three hydrogels was (8.82 ± 0.05), meeting the requirements for rectal injection (pH 3–10). The moisture retention rate surpassed 90%, showcasing excellent moisture-holding capacity. Additionally, the gel strengths were moderate and suitable for rectal injections. Evaluation of SZ-A release from the hydrogels indicated slow release characteristics at 37 °C, with the cumulative dissolution rate aligning with the dissolution rate, emphasizing that the drug release rate was determined by the gel dissolution rate (Fig. 1F).

The rheological properties of the three thermo-sensitive hydrogels were characterized using a rotational rheometer. The LVR reflected the structural characteristics of the system, describing hydrogel stability. Rheological measurements of the three thermo-sensitive hydrogels revealed no significant differences in the LVR within the 0.1%-100% strain scan range (Fig. 2A). In the frequency scan range of 0.1–10 Hz, the $G'$ values of the three thermo-sensitive hydrogels remained stable, indicating the stability of their internal gel structure. Compared to Gel-2 and Gel-3, Gel-1 exhibited a higher $G'$, signifying a higher elastic modulus (Fig. 2B). This suggests that Gel-1 was less susceptible to deformation or disruption, effectively preserving the gel structure. Additionally, the viscosity of the three thermo-sensitive hydrogels before and after gel transformation was measured. Experimental results indicated that, compared to Gel-2 and Gel-3, Gel-1 had the

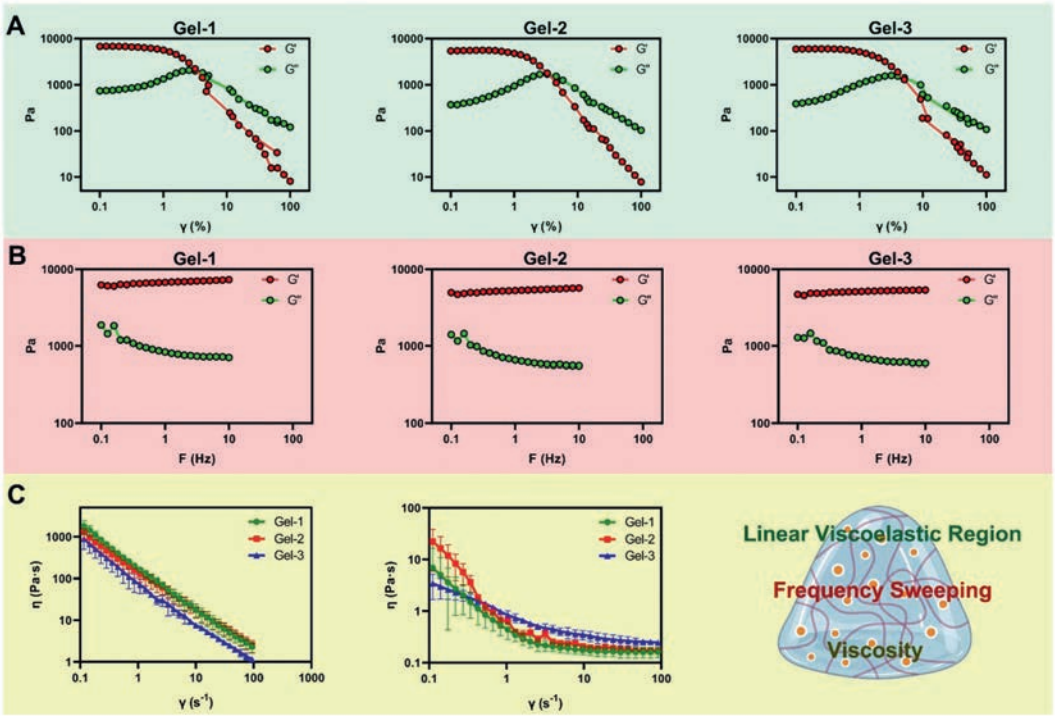


**Fig. 2.** Rheological characterization of different SZ-A hydrogel: (A) Linear viscoelastic region of different SZ-A hydrogel. (B) Frequency scans of different SZ-A hydrogel. (C) The viscosity curves of different SZ-A hydrogels against the shear rate at room temperature and gelling temperature. Data are presents as mean ± SD ($n = 3$).

lowest viscosity before gelation, showcasing better flowability and suitability for rectal administration. Upon reaching the gelation temperature after entering the rectum, Gel-1 exhibited high post-gelation viscosity, enhancing its adhesion to the rectal mucosa (Fig. 2C). Based on these rheological findings, Gel-1 was selected as the optimal hydrogel formulation.

The drug loading of the selected Gel-1 was investigated using rotational rheometry, and the stability of the gel structure was assessed through gel LVR and frequency scanning. Rheological measurements of thermo-sensitive hydrogels with varying drug loadings revealed that, within the 0.1%–100% strain scanning range, the LVR of the hydrogels with 1%–7% drug loading exhibited minimal fluctuation, indicating stable internal structure capable of withstanding significant deformations without damage. However, when the drug loading exceeded 7%, the LVR of the thermo-sensitive hydrogel underwent substantial alterations, with $G'$ showing significant fluctuations, signifying instability and susceptibility to damage (Fig. S1A in Supporting information). In the frequency scanning range of 0.1–10 Hz, $G''$ of the thermo-sensitive hydrogel fluctuated considerably when the drug loading surpassed 5%, indicating instability in the fluid state (Fig. S1B in Supporting information). Furthermore, the pH and gelling temperature of thermo-sensitive hydrogels with different drug loads were measured. The results revealed an increase in pH with rising SZ-A drug loading, while the gelation temperature of the thermo-sensitive hydrogels decreased (Fig. S1B). This observation may be attributed to SZ-A's viscosity, which reduces the gelation temperature. As SZ-A primarily comprises alkaloids, the pH increased with an elevated alkaloid content. Based on these findings, the drug loading capacity of the thermo-sensitive hydrogel was determined to be less than 5%.

The physicochemical characterization of the thermo-sensitive hydrogel with 2% drug loading was meticulously conducted. The rheological test results, as depicted in Fig. S1C (Supporting information), revealed minimal fluctuations in the LVR within the 0.1%–100% strain scan range, indicative of a relatively stable internal structure. Under high strain, both $G'$ and $G''$ dropped synchronously, signifying the shear-thinning property of the thermo-sensitive hydrogel. Within the frequency scan range of 0.1–10 Hz, the hydrogel displayed negligible frequency dependency. Additionally, the viscosity trend with shear rate at 4 °C and body temperature was determined. At 4 °C, the hydrogel exhibited constant viscosity irrespective of changes in shear rate, behaving as a Newtonian fluid. Conversely, at body temperature, the viscosity decreased with increasing shear rate, showcasing shear-thinning behavior. This property aligns with injectable systems and is consistent with the modulus results, illustrating the transition from liquid to solid and confirming the phase transition of thermo-sensitive hydrogels.

The formation of thermo-sensitive hydrogels was assessed using Fourier transform infrared spectroscopy (FT-IR), and the obtained spectra are presented in Fig. S1D (Supporting information). Characteristic peaks of SZ-A at 2894 and 1644 $cm^{-1}$ weakened upon interaction with the polymer materials. The experimental results suggest that SZ-A not only mixed but interacted with the polymer materials, being enveloped by them. Fig. S1D displays the differential scanning calorimeter (DSC) spectra of SZ-A, the blank hydrogel, and the thermo-sensitive hydrogel. SZ-A and the blank hydrogel exhibited broad endothermic peaks at 100.3 and 103.6 °C, respectively, attributed to water evaporation. SZ-A displayed a distinct, narrow endothermic peak at 104.3 °C. However, in the thermo-sensitive hydrogel, no corresponding peak for SZ-A was observed, indicating SZ-A's interaction with the polymer materials and dispersion in an amorphous state within them. This observation aligns with the FT-IR results.

Male Sprague–Dawley rats weighing 160–180 g were procured from Huafukang Biotechnology Co., Ltd. (Beijing, China). Institutional Animal Care and Use Committee approval was obtained for all animal experiments conducted at Peking Union Medical College, and the rats were housed in a specific pathogen-free environment.

To evaluate the effectiveness of the prepared thermo-sensitive hydrogel in extending the retention duration of SZ-A in the colon, both free SZ-A aqueous solution and SZ-A hydrogel were labeled with IR-820 and utilized for *in vivo* imaging of small animals to

monitor the retention period in the colon following rectal administration. The experimental results are presented in Fig. S2A (Supporting information). Within 0.5 h, the fluorescence intensity in both the rectally administered and fluorescently labeled hydrogel groups surpassed that in the orally administered free IR-820 group. This suggests that IR-820 can rapidly localize in the colon following rectal administration, releasing the fluorescent dye to exert a local targeting effect. As time progressed, the fluorescence intensity of the rectally administered group weakened, whereas the fluorescently labeled hydrogel group maintained a strong fluorescence intensity, indicating that the hydrogel could continuously localize at the colonic site, interact with colonic epithelial cells, and slowly release fluorescent dyes to exert a local effect. Even 5 h after rectal instillation, the orally free IR-820, and rectally administered groups showed only weak fluorescence signals, whereas the thermo-sensitive hydrogel group maintained a strong fluorescence signal. The semi-quantitative statistical results of the ROI values are shown in Fig. S2B (Supporting information), and similar conclusions were drawn from the *in vivo* imaging observations of small animals. The experimental results demonstrated that the fluorescently labeled gel could rapidly localize in the colon after rectal administration, sustaining retention and slow release of the fluorescent dye compared to the oral and rectal administration groups, which may be highly beneficial in maintaining an effective drug concentration in the colon over the long term.

To assess the *in vivo* biocompatibility of the thermo-sensitive hydrogel prepared after rectal administration, a continuous 7-day rectal irritation test was conducted. Evaluation criteria included hematoxylin-eosin (HE) staining and the levels of key inflammatory factors in the plasma and colonic tissues. After a 7-day administration period, the rectal tissues in the thermo-sensitive hydrogel group exhibited no discernible pathological alterations, such as redness, swelling, or mucosal damage, compared to the control group. The results of HE staining, as illustrated in Fig. S2C (Supporting information), indicated that the mucosa, submucosa, muscular layer, and outer membrane structures in the normal group were intact. Most intestinal structures in the normal saline group showed no apparent abnormalities. Minimal neutrophil infiltration was observed in the mucosal layer, and the glandular structures exhibited regular and intact shapes. The majority of intestinal structures in the thermo-sensitive hydrogel group showed no apparent abnormalities. Isolated neutrophil infiltration was observed in the mucosal layer and was extensively distributed. Additionally, there was a minor presence of inflammatory cell infiltration in the mucosal layer, but it was very slight. The levels of some important inflammatory factors in the plasma and colonic tissue were also measured, and the results are shown in Fig. S2D (Supporting information). The levels of important inflammatory factors in the plasma and colonic tissue in the thermo-sensitive hydrogel group did not change significantly compared to those in the normal (Nor) and normal saline (NS) groups ($P > 0.05$). The experimental results showed no significant difference between the groups, indicating that the SZ-A thermo-sensitive hydrogel had no obvious mucosal irritation or high biological risk *in vivo*.

The irritation of the rectal mucosa caused by the warming gel is an important indicator for the safety evaluation of rectal warming gel [40]. Although P407 has been approved by the Food and Drug Administration (FDA) as an excipient for injectable drugs, its *in vitro* safety is yet to be assessed. It has been demonstrated that even a 20% concentration of P407 hydrogel, when applied daily to the dorsal skin of C57BL/6 mice for 5 days, did not result in any observable clinical signs of toxicity [41].

The TNBS-anhydrous ethanol model is a simple, economical, and feasible approach that is well-suited for evaluating and investigating drugs for the prevention and treatment of UC [42]. Consequently, this study assessed the *in vivo* therapeutic effectiveness of the SZ-A thermo-sensitive hydrogel in a rat model of UC induced by TNBS/anhydrous ethanol. After 1 day of TNBS/anhydrous ethanol modeling, rats displayed symptoms such as decreased activity, reduced appetite, depressive behavior, and the presence of blood in the stool. These symptoms are commonly associated with acute UC in rats. Following the modeling, the body weight of the control group rats exhibited a consistent increase, while the other groups demonstrated a comparatively slower rate of weight gain than the control group. By the conclusion of the experiment, the model group exhibited the lowest body weight, while the other four groups demonstrated a trend towards some degree of remission. Among these, the group administered with the positive drug salicylazosulfapyridine (SASP) and the SZ-A hydrogel group (34 mg/kg) showed a more significant improvement in weight trends in UC rats (Fig. 3A), suggesting a gradual restoration of intestinal function in these two groups.

At the end of the experiment, the rat colons were removed, photographed, and measured (Fig. 3B). It is evident from the figures that the model group displayed changes, such as colonic atrophy and edema, in comparison with the control group, indicating the successful induction of colitis. To a certain extent, each treatment group tended to maintain the length of the rat colon, especially the SASP and SZ-A hydrogel groups (17 mg/kg), which exhibited significantly longer colons compared to the oral administration group (Fig. 3C). This suggests that the SZ-A hydrogel can alleviate colon atrophy and edema resulting from UC. To some extent, its efficacy was superior to oral administration, and it could better maintain colon length.

To assess the effects of TNBS/anhydrous ethanol-induced modeling on UC inflammation infiltration, the concentrations of TNF-$\alpha$, TGF-$\beta$1, IL-1$\beta$, IL-6, and IL-18 in colonic tissues were quantified using enzyme-linked immunosorbnent assay (ELISA). As shown in Fig. 3D, the severity of inflammation may be associated with pro-inflammatory cytokine levels. In the colonic tissues of all groups, the model group exhibited the highest expression of inflammatory factors compared to the blank control group. Following treatment with SZ-A or SZ-A hydrogel, the levels of inflammatory cytokines, including IL-1$\beta$, TNF-$\alpha$, IL-6, and IL-18, were down-regulated, indicating a reduction in colonic inflammation. Compared with the model group, the remaining treatment groups alleviated, to some extent, the impact of inflammatory infiltration caused by UC. Significantly, compared to the SZ-A oral administration group, the SZ-A hydrogel group exhibited lower levels of pro-inflammatory cytokines, indicating that the SZ-A hydrogel was more effective in suppressing the inflammatory response induced by TNBS/anhydrous ethanol.

Moreover, the myeloperoxidase (MPO) activity in colonic tissues from each group was measured after treatment. As depicted in Fig. 3D, the model group demonstrated notably elevated levels of colonic MPO ($P < 0.01$). In contrast, the MPO levels in the other treatment groups showed a significant reduction ($P < 0.05$).

To further examine the inflammation of the colonic mucosa in each group, we assessed colonic tissue sections stained with HE. As depicted in Fig. 3E, the model group exhibited inflammation characterized by significant mucosal damage when compared to the normal group. There was an evident infiltration of inflammatory cells in the submucosal layer, accompanied by mucosal layer defects and ulcerations. In the SASP group, there was minimal infiltration of inflammatory cells and the damaged colonic morphology exhibited effective repair. After oral treatment with SZ-A and SZ-A hydrogels, improvements in the colonic damage caused by UC were evident, with some colonic segments approaching a normal appearance. This indicated that all treatment groups ameliorated the symptoms of UC.

A reduction in tight junction (TJ) proteins can impair colonic barrier function. Intestinal epithelial cells linked by TJ proteins,

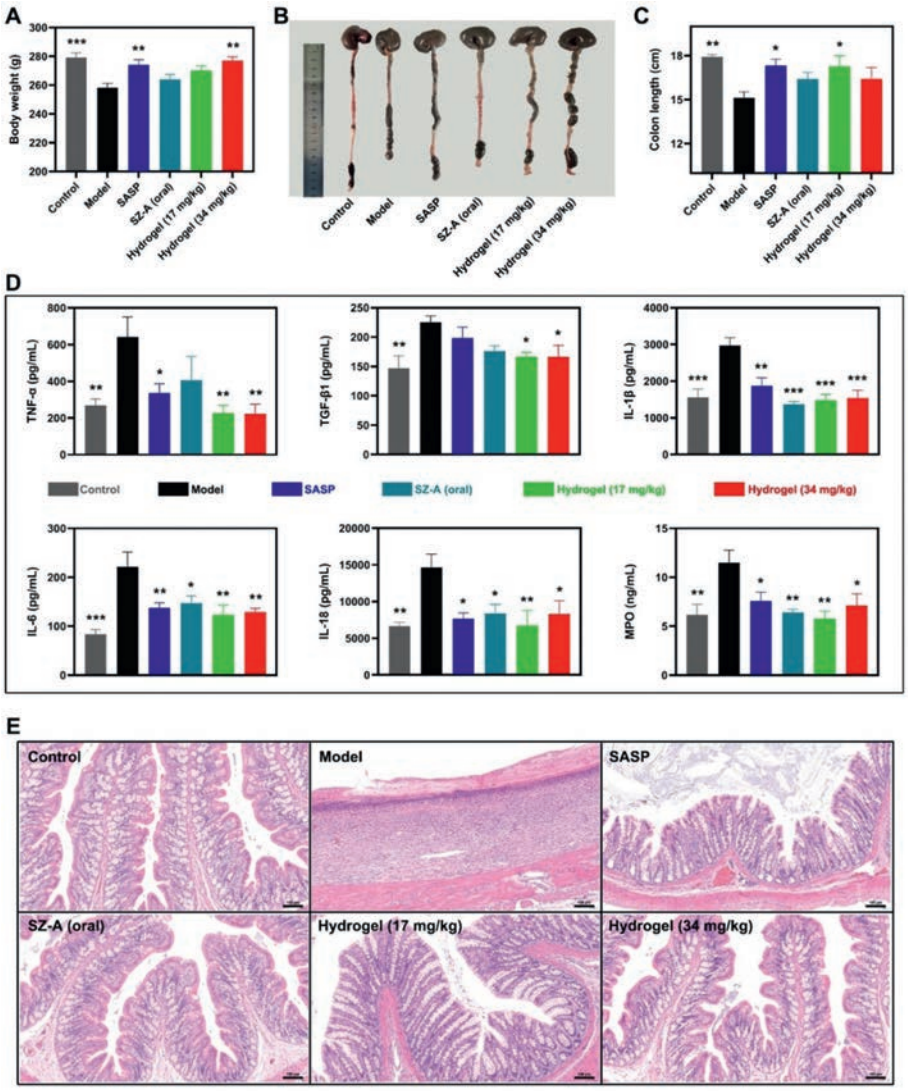


**Fig. 3.** The therapeutic effects of thermos-sensitive SZ-A hydrogel on TNBS/ anhydrous ethanol-induced UC rats: (A) The weight of the rats at the end point of treatment. (B) The colonic appearance of rats at the end point of treatment. (C) The colon length after treatment. (D) Histogram analysis of rats colonic inflammatory cytokine changes after treatment. (E) HE staining, scale bar: 100 μm. Data are presents as mean ± standard error of mean (SEM) ($n = 6$). $^{*}P < 0.05$, $^{**}P < 0.01$, $^{***}P < 0.001$, compared to model group.

including zonula occludens-1 (ZO-1) and claudin-1, prevent ions and small molecules from freely passing through the space between two epithelial cells [43,44]. To elucidate the impact of SZ-A hydrogel on colonic mucosal damage in UC rats, the expression of ZO-1 and claudin-1 was assessed using immunohistochemistry. As depicted in Figs. S3A and B (Supporting information), immunohistochemical staining for ZO-1 and claudin-1 showed greater immunoreactivity in the normal control group and various treatment groups than in the model group.

This study meticulously examined and compared the effects of different treatments in alleviating colonic inflammation and restoring the intestinal mucosal barrier. Compared to the model group, both the SZ-A and SZ-A hydrogel groups displayed an effective trend in mitigating inflammation. Furthermore, certain forms of poloxamers exhibited anti-inflammatory properties, such as P188, which may play a crucial role in preventing environmental toxin damage and improving neuroinflammation-mediated cognitive deficits in Parkinson's disease (PD) [45].

To assess the *in vitro* biocompatibility of the SZ-A thermosensitive hydrogel, the influence of different concentrations of the SZ-A hydrogel extract and different concentrations of SZ-A on cell viability was examined (Fig. S4A in Supporting information). The biocompatibility of different concentrations of SZ-A was tested using a calcein-AM/propidium iodide (PI) cell viability/cytotoxicity assay (Fig. S4B in Supporting information). The results indicate that, in comparison to the normal group, the proliferation of Raw264.7 cells was not significantly affected by various concentrations of SZ-A, demonstrating excellent biocompatibility.

As the key immune cells in the intestine, macrophages play an important role in maintaining intestinal homeostasis and tissue repair in UC [46]. Raw264.7 cells were polarized through lipopolysaccharide (LPS, 1 μg/mL) activation to investigate the impact of SZ-A on modulating inflammatory responses. The influence of various concentrations of SZ-A on intracellular nitric oxide (NO) induced by LPS was assessed using the classical Griess Reagent method. Furthermore, the levels of TNF-$\alpha$, IL-6, and IL-1$\beta$ secretion in LPS-induced Raw264.7 cells at varying concentrations of SZ-A were evaluated using ELISA. The experimental findings, illustrated in Fig. S4C (Supporting information), demonstrated a notable elevation in intracellular NO content in the LPS model group compared to the blank control group. In contrast, varying concentrations of SZ-A led to a significant reduction in NO levels compared to those observed

in the model group. Moreover, in comparison to the control group, the model group exhibited an increased secretion of inflammatory mediators, such as TNF-$\alpha$, IL-6, and IL-1$\beta$, into the supernatant of the cell culture. Nevertheless, the treatment of Raw264.7 cells with SZ-A reduced this increase, with a more pronounced anti-inflammatory effect observed at higher concentrations. The findings suggest that SZ-A can suppress the inflammatory reaction in LPS-induced Raw264.7 macrophages.

In this study, we successfully developed a rectal drug delivery-targeting formulation, namely, SZ-A thermo-sensitive hydrogel, using a combination of thermo-sensitive materials, modulators, and bioadhesive agents. This formulation aims to enhance adhesiveness and injectability for managing UC. The thermo-sensitive gel remains in a liquid state at room temperature and transitions to a semi-solid state upon reaching its gelation temperature. Rheological experiments revealed its viscoelastic properties and shear-thinning behavior. The pH level, moisture retention capacity, and gel strength all meet the criteria for rectal drug delivery formulations. Both *in vitro* drug release and *in vivo* targeting experiments suggest that the thermo-sensitive gel outperforms conventional enema solutions, demonstrating a significant sustained-release effect. It extends the drug's residence time in the colon, facilitating continuous drug release. *In vivo* experiments on mucosal irritation demonstrate the safety and non-irritating nature of the gel when applied to the colon. The TNBS/ethanol modeling method, considered ideal for studying inflammatory bowel disease, shows promising results *in vivo* efficacy experiments. The SZ-A thermo-sensitive hydrogel maintains colon length, regulates body weight, and decreases the expression of pro-inflammatory factors. *In vitro* cytological experiments indicate that SZ-A in different dosage groups does not significantly inhibit cell proliferation, showcasing excellent biocompatibility. In summary, rectal thermo-sensitive hydrogels combine the advantages of both solution and gel formulations, enhancing drug absorption and local tissue drug concentrations. This leads to improved medication compliance and clinical efficacy, presenting potential applications in various therapeutic scenarios.

However, the study had limitations. Rectal drug administration may have posed challenges to patient compliance. Additionally, an in-depth exploration of the anti-inflammatory mechanism of SZ-A thermo-sensitive hydrogel is lacking. Future studies should focus on developing advanced, easy-to-administer rectal pusher devices and employing pharmacological techniques, such as multi-omics analysis, to delve deeper into the specific mechanisms and targets responsible for the therapeutic effects of SZ-A thermo-sensitive hydrogel in UC.

## Declaration of competing interest

The authors declare that they have no known competing financial interests or personal relationships that could have appeared to influence the work reported in this paper.

## Acknowledgments

This work was financially supported by the National Natural Science Foundation (No. 82304393, China), Beijing Nova Program (Nos. Z211100002121127 and 20220484219, China), Beijing Natural Science Foundation (No. L212059, China), and CAMS Innovation Fund for Medical Sciences (No. 2021-I2M-1-028, China).

## Supplementary materials

Supplementary material associated with this article can be found, in the online version, at doi:10.1016/j.cclet.2024.109736.

## References

[1] Y. Liu, B.G. Li, Y.H. Su, et al., J. Ethnopharmacol. 289 (2022) 115084.
[2] D. Muthas, A. Reznichenko, C.A. Balendran, et al., Scand J. Gastroenterol. 52 (2017) 125–135.
[3] H. Shi, X. Zhao, J. Gao, et al., Chin. Chem. Lett. 31 (2020) 3102–3106.
[4] T. Kucharzik, S. Koletzko, K. Kannengiesser, A. Dignass, Dtsch. Arztebl Int. 117 (2020) 564–574.
[5] T. Kobayashi, B. Siegmund, C. Le Berre, et al., Nat. Rev. Dis. Prim. 6 (2020) 74.
[6] Z. Liu, H. Liu, J. Cheng, et al., Chin. Chem. Lett. 35 (2024) 109074.
[7] Y. Ye, Z. Pang, W. Chen, S. Ju, C. Zhou, Int. J. Clin. Exp. Med. 8 (2015) 22529–22542.
[8] M.F. Neurath, M. Leppkes, Semin. Immunopathol. 41 (2019) 747–756.
[9] R. Ungaro, S. Mehandru, P.B. Allen, L. Peyrin-Biroulet, J.F. Colombel, Lancet 389 (2017) 1756–1770.
[10] S. Danese, G. Roda, L. Peyrin-Biroulet, Nat. Rev. Gastroenterol. Hepatol. 17 (2020) 1–2.
[11] B. Gros, G.G. Kaplan, JAMA 330 (2023) 951–965.
[12] Y. Cui, T. Zhu, X. Zhang, et al., Chin. Chem. Lett. 33 (2022) 4617–4622.
[13] M. Kayal, S. Shah, J. Clin. Med. 9 (2019) 94.
[14] C. Mowat, A. Cole, A. Windsor, et al., Gut 60 (2011) 571–607.
[15] C. Zhang, J. Li, M. Xiao, et al., Chin. Chem. Lett. 33 (2022) 4924–4929.
[16] M. Sun, W. Ban, H. Ling, et al., Chin. Chem. Lett. 33 (2022) 4449–4460.
[17] L. Herrera Estrada, H. Wu, K. Ling, et al., ACS Nano 11 (2017) 9650–9662.
[18] C. Li, Y. Zhao, J. Cheng, et al., Adv. Sci. 6 (2019) 1900610.
[19] Q. Liu, S. Liu, H. Cao, et al., Front. Pharmacol. 12 (2021) 642400.
[20] H. Cao, W. Ji, Q. Liu, et al., J. Ethnopharmacol. 280 (2021) 114483.
[21] L. Qu, X.C. Liang, G.Q. Tian, et al., Chin. J. Integr. Med. 28 (2022) 304–311.
[22] Y.M. Chen, C.F. Lian, Q.W. Sun, et al., Antioxidants 11 (2022) 905.
[23] T.J. Purohit, S.M. Hanning, Z. Wu, Pharm. Dev. Technol. 23 (2018) 942–952.
[24] L.M. Chiang, H.S. Wang, H.H. Shen, et al., Pediatr. Neonatol. 52 (2011) 30–33.
[25] J. Shi, L. Yu, J. Ding, Acta Biomater. 128 (2021) 42–59.
[26] A.D. Drozdov, J.D. Christiansen, J. Mech. Behav. Biomed. Mater. 114 (2021) 104215.
[27] Y. Liu, X. Wang, Y. Liu, X. Di, AAPS PharmSciTech 19 (2018) 338–347.
[28] Y. Chen, J.H. Lee, M. Meng, et al., Materials 14 (2021) 4522.
[29] W. Boonlai, V. Tantishaiyakul, N. Hirun, T. Sangfai, K. Suknuntha, AAPS PharmSciTech 19 (2018) 2103–2117.
[30] B. Shriky, A. Kelly, M. Isreb, et al., J. Colloid Interface Sci. 565 (2020) 119–130.
[31] Y. Petkova-Olsson, C. Oelschlaeger, H. Ullsten, L. Järnström, J. Colloid Interface Sci. 514 (2018) 459–467.
[32] I. Jarak, C.L. Varela, E. Tavares da Silva, et al., Eur. J. Med. Chem. 206 (2020) 112526.
[33] M.I. Malik, S. Lee, T. Chang, J. Chromatogr. A 1442 (2016) 33–41.
[34] P. Xue, L. Wang, J. Xu, et al., Int. J. Pharm. 589 (2020) 119846.
[35] S.J. Buwalda, K.W. Boere, P.J. Dijkstra, et al., J. Control. Release 190 (2014) 254–273.
[36] J. Wu, J. Zhu, C. He, et al., ACS Appl. Mater. Interfaces 8 (2016) 18710–18721.
[37] S. Rençber, S.Y. Karavana, Z.A. Şenyiğit, et al., Pharm. Dev. Technol. 22 (2017) 551–561.
[38] S.Y. Karavana, Z.A. Şenyiğit, Ç. Çalışkan, et al., Drug Des. Devel. Ther. 12 (2018) 1959–1975.
[39] M.A. Fathalla, Z.A. Vangala, M. Longman, et al., Eur. J. Pharm. Biopharm. 114 (2017) 119–134.
[40] E. Ban, C.K. Kim, Arch. Pharm. Res. 36 (2013) 586–592.
[41] S. Yogev, A. Shabtay-Orbach, A. Nyska, B. Mizrahi, Toxicol. Pathol. 47 (2018) 426–432.
[42] T. Karaca, Y.H. Uz, S. Demirtas, I. Karaboga, G. Can, Iran. J. Basic Med. Sci. 18 (2015) 370–379.
[43] G. Wang, Q. Li, D. Chen, et al., Theranostics 9 (2019) 6191–6208.
[44] J. Wang, C. Zhang, C. Guo, X. Li, Int. J. Mol. Sci. 20 (2019) 5751.
[45] W. Ding, H. Lin, X. Hong, D. Ji, F. Wu, Toxicology 436 (2020) 152437.
[46] E. Wang, R. Han, M. Wu, et al., Chin. Chem. Lett. 35 (2024) 108361.